ELSEVIER

Microporous and Mesoporous Materials 39 (2000) 457–463

MICROPOROUS AND MESOPOROUS MATERIALS

www.elsevier.nl/locate/micromeso

para-Selective *t*-butylation of phenol over mesoporous H-AlMCM-41

A. Sakthivel, S.K. Badamali, P. Selvam *

Department of Chemistry, Indian Institute of Technology Bombay, Powai, Mumbai 400 076, India

Received 24 December 1999; accepted 22 March 2000

Abstract

Vapour phase alkylation of phenol with *t*-butyl alcohol (2-methyl-2-propanol) was carried out over mesoporous H-AlMCM-41 in the temperature range 448–498 K. In this reaction, *p*-*t*-butyl phenol was obtained as a major product with high selectivity. While the phenol conversion increases with a decrease in phenol-to-*t*-butyl alcohol ratio, the catalytic activity decreases with time-on-stream due to deactivation of the catalyst. At higher temperatures, both the *ortho*- and *para*-isomers, viz., *o*-*t*-butyl phenol and *p*-*t*-butyl phenol, undergoes isomerization leading to *m*-*t*-butyl phenol.

Keywords: Mesoporous molecular sieves; H-AlMCM-41; Butylation of phenol; *p*-*t*-Butyl phenol

1. Introduction

para tertiary Butyl phenol (*p*-*t*-BP) finds an increasing use in the manufacture of phenolic resins, antioxidants, polymerization inhibitors, lube additives as well as in the production of substituted triaryl phosphates [1]. Numerous studies have been reported on the *t*-butylation of phenol, both in homogeneous and heterogeneous using several acid catalysts, viz., sulfuric acid, phosphoric acid, arene sulfonic acid, alumina silca supported, clay, cation exchange resins, microporous molecular sieves, etc. [2–26]. However, the homogeneous catalysts have difficulties such as hazardous nature and tedious work-up for the separation of catalyst. On the other hand, the cationic exchange resins cannot be used at higher temperatures. Therefore, in recent years considerable attention has been made using heterogeneous catalysts [16,20,25,26].

The presence of phenolic (–OH) group kinetically favours *o*-alkylation [2,3]. However, due to steric hindrance, thermodynamically unfavoured *o*-isomer, viz., *ortho tertiary* butyl phenol (*o*-*t*-BP) readily isomerizes into less hindered, partially kinetically favourable *p*-isomer [2–6]. Further, in this reaction, the selectivity of the product depends on the nature of the acidic sites present in the catalysts as well as the reaction temperature [16,20,25–30]. A schematic representation of the reaction is given in Fig. 1. As can be seen from Fig. 1, the weak acidic catalyst, e.g., Na^+ and K^+ ion-exchanged zeolite-Y leads to oxygen alkylated product (phenyl alkyl ether, *t*-BPE) as a major product [5,16]. The strong acidic catalyst-like zeolite-β [31], or at high temperatures the reaction produces carbon alkylated product, viz., *m*-*t*-butyl phenol (*m*-*t*-BP).

* Corresponding author. Fax: +91-22-576-7152.
E-mail address: selvam@chem.iitb.ernet.in (P. Selvam).

1387-1811/00/$ - see front matter
PII: S1387-1811(00)00222-5

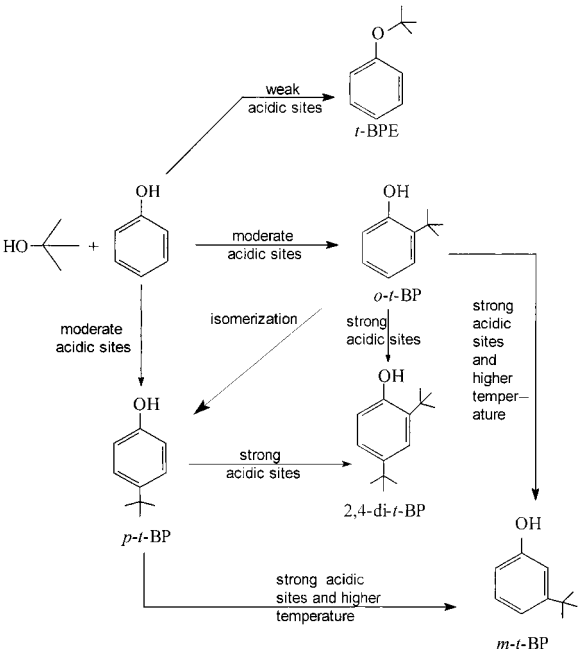

Fig. 1. Effect of acid sites on the alkylation of phenol with *t*-butyl alcohol.

This is formed by the secondary isomerization of initially formed *o*- and *p*-isomers [27–31]. On the other hand, the moderate acidic catalysts, such as ZSM-12 [20], SAPO-11 [25] and zeolite-Y [16,30], are suitable for the formation of *p*-isomer. In this regard, it is interesting to note that the aluminium analogue of the recently discovered mesoporous (silicate) MCM-41, i.e. AlMCM-41, [32–34] has moderate acidity in addition to its high surface area and (meso) pore size, which may be advantageous for the chosen reaction. Therefore, in the present study, we have used the protonated AlMCM-41 catalyst, viz., H-AlMCM-41, for the vapour phase *t*-butylation of phenol.

2. Experimental

2.1. Synthesis

Aluminium sulphate (SDs: 98%), fumed silica (Aldrich: 99.8%) and cetyltrimethylammonium bromide (CTAB, Aldrich: 99%) were used as sources for aluminium, silicon and template, respectively. Tetramethylammonium hydroxide (TMAOH, Aldrich: 25 wt.%) and sodium hydroxide (Loba: 98%) were used as organic base and alkali sources. The Na^+ form of AlMCM-41 was prepared, according to a similar procedure described in the literature [35], with synthesis gel having a chemical (molar) composition of $2SiO_2$:$0.27(CTA)_2O$:$0.26Na_2O$:$0.26(TMA)_2O$:$0.017Al_2O_3$:$120H_2O$. The typical synthesis procedure is as follows: first TMAOH was dissolved in water and stirred for 5 min. To this, fumed silica was added slowly and the resulting solution is designated as A. Another solution, B, was prepared by mixing CTAB and NaOH in distilled water and stirred for about 30 min. Both these solutions, viz., A and B, were mixed together and a gel was formed. Then, the aluminium sulphate in water was added slowly to the above gel and was stirred for an hour for homogenization. The final gel pH was adjusted to 11.5 and was transferred into teflon-lined stainless steel autoclaves. The reaction vessel was kept in an air oven for crystallization at 373 K for 24 h. The solid product obtained was washed, filtered and dried overnight at 373 K. The resulting (as-synthesized) AlMCM-41 sample was then calcined at 823 K in nitrogen for 3 h followed by in air for 9 h at a heating rate of 2 K min^{-1}. This sample is denoted as-calcined (Na^+ form) AlMCM-41.

2.2. Preparation of acid catalyst

The acid form of AlMCM-41 was prepared from the Na^+ form of AlMCM-41 as per the procedure described elsewhere [31]. First, NH_4^+ form of AlMCM-41 was obtained by repeated exchange of Na^+ form of AlMCM-41 with 1 M NH_4NO_3 at 353 K for 6 h. The protonated form of the catalyst, i.e. H-AlMCM-41, was obtained by deammoniation of NH_4^+ form of the catalyst at 773 K for 6 h.

2.3. Characterization

All the samples, viz., as-synthesized, calcined, ammonium ion exchanged and protonated AlMCM-41, were characterized systematically by powder X-ray diffraction (XRD: Rigaku), simul-

taneous thermogravimetry-differential thermal analysis (TG-DTA: DuPont), BET surface area (Smartsorb 90), elemental analysis by inductively coupled plasma-atomic-emission spectroscopy (ICP-AES, Labtam Plasma 8440) and ^{27}Al magic angle spinning nuclear magnetic resonance (MAS-NMR, Varian) spectroscopy.

2.4. Temperature programmed desorption of ammonia

The acidic behaviour of H-AlMCM-41 was followed by the temperature programmed desorption of ammonia (TPDA) as per the procedure described elsewhere [31]. About 200 mg of the protonated sample was placed in quartz reactor and was activated at 773 K in air for 6 h followed by 2 h in helium (with a flow rate of 50 ml min^{-1}). Then the reactor was cooled to 373 K and maintained for another hour under the same condition. Ammonia adsorption was carried out by passing the gas through the sample for 15–20 min at this temperature. Subsequently, it was purged with helium for an hour to remove the physisorbed ammonia. The desorption of ammonia was carried out by heating the reactor up to 873 K at the rate of 10 K min^{-1} using a temperature programmer (Eurotherm). The amount of ammonia desorbed was estimated with the aid of thermal conducting detector (TCD) response factor for ammonia.

2.5. Reaction

The *t*-butylation of phenol was carried out using 750 mg of H-AlMCM-41 catalyst in a fixed-bed flow reactor. The catalyst was activated at 773 K in a flow of air for 8 h followed by cooling to reaction temperature (448–498 K) in nitrogen atmosphere. After an hour, the reactant mixture, viz., phenol and *t*-butyl alcohol, with a desired ratio and weight hour space velocity (WHSV) was fed into the reactor using a liquid injection pump (Sigmamotor) and nitrogen as the carrier gas. The gaseous products were cooled and the condensed liquid products were collected at every 30 min interval. The products, viz., *p*-*t*-BP, *o*-*t*-BP and 2,4-di-*t*-butyl phenol (2,4-Di-*t*-BP), were identified by gas chromatography (NUCON 5700) with SE-30 column while *m*-*t*-BP was identified by employing AT1000 column. Further, the products were confirmed using a combined gas chromatography–mass spectrometry (GC–MS; HEWLETT G1800A) with HP-5 capillary column.

3. Results and discussion

Shown in Fig. 2 are the powder XRD patterns of both as-synthesized and calcined AlMCM-41 catalyst. The diffraction patterns are characteristics of typical mesoporous MCM-41 structure [37,38]. As can be seen from the figure that the (1 0 0) reflection of AlMCM-41 is shifted to higher values ($d_{100} = 41.64$ Å) compared to its siliceous analogue, MCM-41 ($d_{100} = 38.78$ Å) which is in agreement with Borade and Clearfield [35]. Thus, suggesting the framework substitution of aluminium in MCM-41 structure as the crystal radius of trivalent aluminium (0.53 Å) is much larger than tetravalent silicon (0.40 Å) in tetrahedral coordination [39]. However, upon calcination the reflections, in general, are shifted towards the lower *d* values to a smaller extent (or higher 2θ values) implying a shrinkage in the unit cell as a result of the removal of (template) surfactant molecules. Further, the XRD patterns of ammonium ion

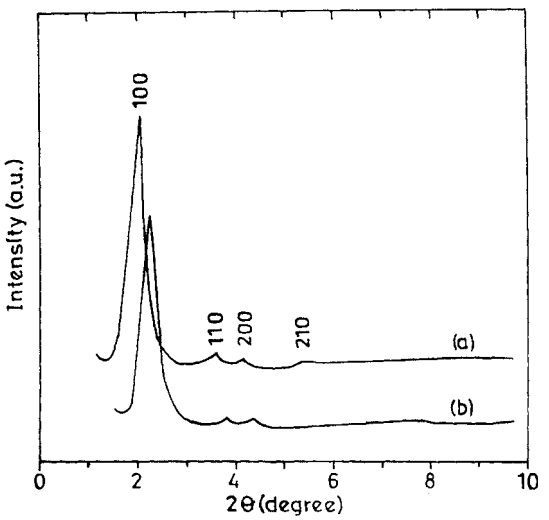

Fig. 2. XRD patterns of (a) as-synthesized and (b) calcined AlMCM-41.

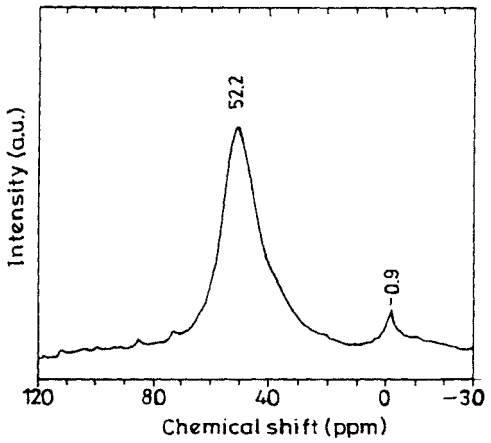

Fig. 3. ^{27}Al MAS-NMR spectrum of calcined AlMCM-41.

exchange and protonated forms of AlMCM-41 also showed clear reflections (not reproduced here) indicating the stability of the materials even after the various treatments. The observed weight loss of ~51% TG for the as-synthesized sample and the BET surface area of ~775 $m^2 g^{-1}$ for the calcined sample further suggest the mesoporous nature of the catalyst [40]. The ICP-AES analysis of calcined AlMCM-41 shows that the Si/Al ratio of the sample is 56, which is close to the initial ratio (Si/Al = 60) in the gel. The ^{27}Al MAS-NMR spectrum (Fig. 3) of the calcined sample exhibit a peak at 52 ppm characteristic of trivalent aluminium in the tetrahedral framework [41]. A weak signal at −0.9 ppm, however, appears due to octahedral aluminium, which may probably be generated during calcination. However, the MAS-NMR results of ammonium ion exchanged and protonated AlMCM-41 (not reproduced here) indicated no further dealumination from the samples.

Fig. 4 depicts the acid sites distribution in H-AlMCM-41 determined by TPDA measurement. It is to be noted here that the desorption of ammonia (a broad peak with a long tail) from different acid sites depends on desorption temperatures [32,33]. Since the AlMCM-41 posses different acid sites, and the desorption temperature are very closely spaced, the peak was not very well separated. However, by changing the experimental conditions, e.g., lowering the heating rate of the desorption process, this may be resolved. Thus, the

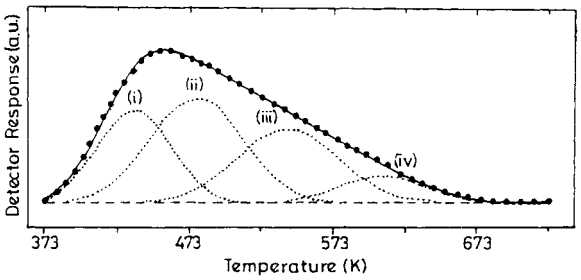

Fig. 4. TPDA profile over H-AlMCM-41.

TPDA peak was deconvulated by using Gaussian function [42] by varying the temperature. This results in four peaks with maxima (T_{max}) at 433, 481, 543 and 609 K. The first three peaks are, respectively, assigned to weak, moderate and strong acid sites [32,33,36,40,43]. The weak acid sites at 433 K are attributed to surface hydroxyl groups, whereas two other peaks at 481 and 543 K originate from moderate and strong structural (Brønsted) acid sites owing to the presence of trivalent aluminium in the framework positions. The broad peak at $T_{max} = 609$ K may arise from (weak) Lewis acid sites. In addition, appearance of a peak at 754 K (not reproduced here) could be due to tricoordinated trivalent aluminium (strong Lewis) sites, which are generated during calcination. It is, however, clear from the figure that the area under profile corresponding to the moderate and strong Brønsted acid sites is much larger which may be useful for the chosen reaction. This is in good agreement with Pu et al. [34].

Table 1 summarizes the results of butylation reaction carried out with various phenol-to-*t*-butyl alcohol ratios. In all the cases, *p*-*t*-BP was obtained as the major product along with small amounts of *o*- and *m*-alkylated products. In addition, trace amount of 2,4-di-*t*-BP was also observed. Unlike zeolite-β [26], the decrease in *t*-butyl alcohol content in the reaction mixture leads to a very small amount of 2,4-di-*t*-BP due to a relatively small amount of strong structural acid sites in H-AlMCM-41. Further, it is also clear from Table 1 that a decrease in phenol-to-*t*-butyl alcohol ratio increases the phenol conversion. It was demonstrated earlier [25,27] that the polar molecule, such as methanol and higher alcohols compete with

Table 1
Tertiary butylation of phenol over H-AlMCM-41 catalyst[a]

Phenol:*t*-butyl alcohol	4:1	2:1	1:1	1:2	1:3	1:4
Product distribution (wt.%)						
Phenol	82.5	69.0	68.4	64.1	58.5	52.5
o-*t*-BP	1.2	2.5	2.6	2.9	3.7	6.0
m-*t*-BP	1.5	2.0	1.4	1.7	1.7	1.7
p-*t*-BP	14.8	26.1	26.6	29.9	34.6	38.0
2,4-Di-*t*-BP	–	0.43	0.95	1.4	1.5	1.8
Phenol conversion (wt.%)	17.5	31.0	31.6	35.9	41.5	47.5
Selectivity (%)						
o-*t*-BP	6.8	8.1	8.3	8.1	8.9	12.6
m-*t*-BP	8.6	6.4	4.4	4.7	4.1	3.6
p-*t*-BP	84.6	84.2	84.5	83.4	83.3	80.0
2,4-Di-*t*-BP	–	1.3	3.1	3.9	3.6	3.7

[a] Reaction conditions: temperature 448 K, WHSV = 4.8 h^{-1}, TOS = 60–90 min.

phenol for the adsorption sites, and with increasing molar excess of the alkylating agent, the phenol conversion increases as also observed in the present study. However, the selectivity to *p*-*t*-BP decreased and that to 2,4-di-*t*-BP increased. Hence, for further studies, viz., effect of temperature and WHSV, an optimum molar fed mixture (phenol: *t*-butyl alcohol) of 2:1 molar ratio was chosen. Fig. 5 shows the effect of time-on-stream on phenol conversion. As can be seen from the figure that up to 90 min, there is an appreciable decrease in phenol conversion which may be possibly due to deactivation of the catalyst.

The influence of temperature on the *t*-butylation reaction at WHSV = 4.8 h^{-1} is shown in Fig. 6. It is evident from the figure that the reaction gives *p*-selective product with good yield at 448 K. But at higher temperatures, a possible isomerization of *o*- and *p*-products leads to thermodynamically favourable *m*-isomer. A similar observation was made by Namba et al. [30] for zeolite-Y. Moreover, the phenol conversion was decreased

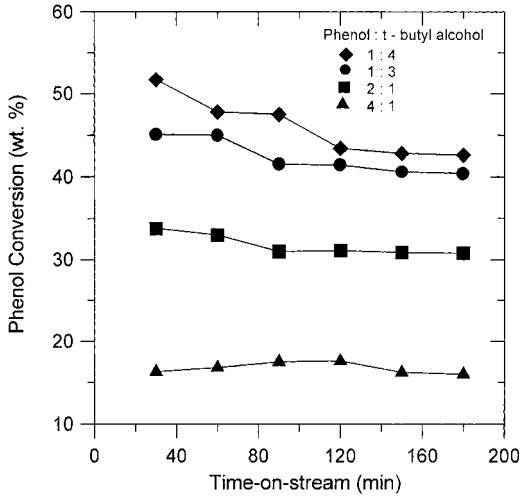

Fig. 5. Effect of time-on-stream on the conversion of phenol over H-AlMCM-41.

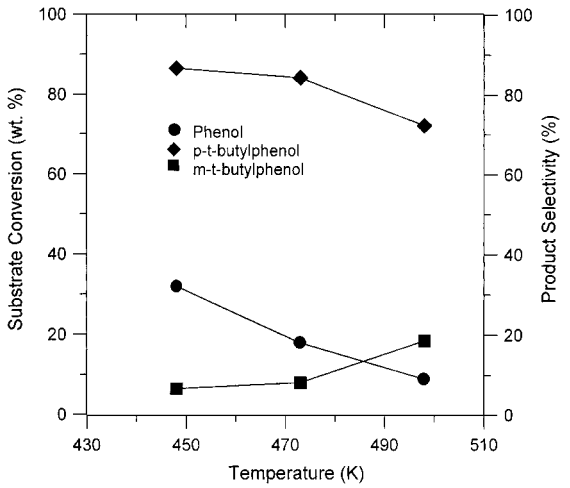

Fig. 6. Effect of temperature on *t*-butylation of phenol over H-AlMCM-41.

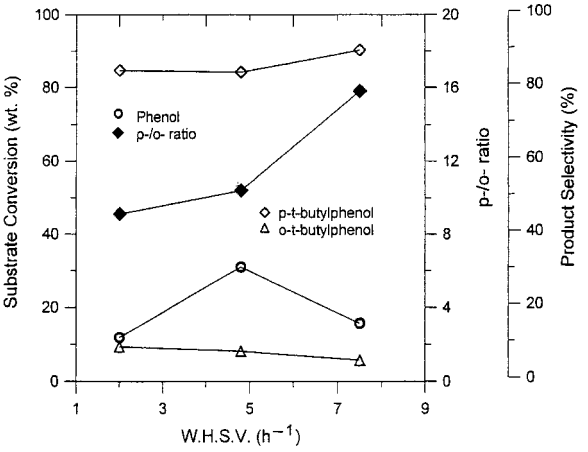

Fig. 7. Effect of space velocity on *t*-butylation of phenol over H-AlMCM-41.

with increase in temperature, which was due to the side reaction (oligomerization) of *t*-butyl alcohol. The results are in agreement with Liu et al. [44] for the *t*-butylation of naphthalene reactions. The reaction was also carried out at different space velocities at 448 K and the results are presented in Fig. 7. It can be seen from the figure that the selectivity of *p*-*t*-BP was higher at 7.5 h^{-1} but with a lower conversion. The reduction in the conversion may simply be due to high diffusion of the reactant molecules at higher space velocity. On the other hand, the low conversion at lower space velocity could be attributed to the dealkylation of BP-to-phenol and coke formation due to longer contact time of the catalyst. The dealkylation of BP-to-phenol was reported earlier at higher temperature [25]. However, GC–MS results showed small amount of dimeric product of butene indicating that the excess *t*-butyl alcohol was converted into butene and its dimeric products.

4. Conclusions

The *t*-butylation reaction of phenol over mesoporous H-AlMCM-41 catalyst indicates that under optimum conditions (phenol:*t*-butyl alcohol = 2:1, $T = 448$ K, WHSV = 4.8 h^{-1}) higher substrate conversion and *para* selectivity can be obtained compared to the microporous catalysts, e.g., SAPO-11, ZSM-12, zeolite-β and zeolite-Y. Moderate-to-strong acidity, large surface area and mesoporous nature of the H-AlMCM-41 may be responsible for the observed results.

Acknowledgements

We thank Dr. P. Veluchamy, Gifu University for XRD and RSIC, IIT Bombay for TG-DTA and GC–MS measurements.

References

[1] A. Knop, L.A. Pilato, Phenolic Resins Chemistry, Springer, Berlin, 1985.
[2] A.J. Kolka, J.P. Napolitano, G.G. Elike, J. Org. Chem. 21 (1956) 712.
[3] B. Love, J.T. Massengale, J. Org. Chem. 22 (1957) 642.
[4] E.A. Goldsmith, M.J. Schlatter, W.G. Toland, J. Org. Chem. 23 (1958) 1871.
[5] G.A. Olah (Ed.), Friedel-Grafts and Related Reactions, vol. 2, Part 1, Interscience, New York, 1963, p. 75.
[6] P.S. Belov, V.I. Isagulyants, V.I. Ponamarenko, L.I. Digovets, Neftepererab Neftekhim (Moscow) 4 (1969) 35.
[7] T. Saito, T. Tanno, T. Kurino, JP Patent 74 00823, 1974.
[8] K. Kagami, Y. Takami, JP Patent 75 112325, 1975.
[9] H. Alfirs, G. Boehm, H. Steimer, Braz. Pedido PI 75 05138, 1976.
[10] M. Petro, J. Kalamer, C. zech. 186606 (1978).
[11] M. Petro, J. Kalamer, D. Mravec, J. Herain, E. Stibranyi, I. Simek, Chem. Purm. 28 (1978) 341.
[12] Yokkaichi Chemical Co. Ltd., JP Patent 58 52233, 1983.
[13] Yokkaichi Chemical Co. Ltd., JP Patent 58 52234, 1983.
[14] M. Imanari, H. Iwane, S. Otaka, JP Patent 61 251633, 1986.
[15] R.A. Rajadhyaksha, D.D. Chaudhari, Ind. Eng. Chem. Res. 26 (1987) 1276.
[16] A. Corma, H. Garcia, J. Primo, J. Chem. Res. (S) (1988) 40.
[17] E. Takahashi, T. Itani, JP Patent 61 251633, 1986.
[18] K.G. Chandra, M.M. Sharma, Catal. Lett. 19 (1993) 309.
[19] A.U.B. Queiroz, L.T. Aikawa, French Patent 2694000, 1994.
[20] C.D. Chang, S.D. Hellring, US Patent 5288927, 1994.
[21] M. Yamamoto, A. Akyama, JP Patent 6122639, 1994.
[22] H. Yamamoto, K. Takahashi, M. Okihama, M. Hirai, JP Patent 08 12610, 1996.
[23] M. Yamamoto, T. Mizuno, M. Okihama, JP Patent 09 10597, 1997.
[24] H. Yamamoto, E. Iiizumi, J. Kunitake, JP Patent 09 12497, 1997.
[25] S. Subramanian, A. Mitra, C.V.V. Satyanarayana, D.K. Chakrabarty, Appl. Catal. A 159 (1997) 229.
[26] K. Zang, D. Xu, H. Zhang, S. Lu, C. Huang, H. Xiang, H. Li, Appl. Catal. A 166 (1998) 89.

[27] R.F. Parton, J.M. Jacobs, D.R. Huybrechts, P.A. Jacobs, Stud. Surf. Sci. Catal. 46 (1989) 163.
[28] R.F. Parton, J.M. Jacobs, H.V. Ootehem, P.A. Jacobs, Stud. Surf. Sci. Catal. 46 (1989) 211.
[29] N.S. Chang, C.C. Chen, S.J. Chu, P.Y. Chen, T.K. Chuang, Stud. Surf. Sci. Catal. 46 (1989) 223.
[30] S. Namba, T. Yashima, Y. Itaba, N. Hara, Stud. Surf. Sci. Catal. 5 (1980) 105.
[31] A. Mitra, Ph.D. Thesis, IIT Bombay, 1997, p. 55.
[32] H. Kosslick, H. Landmesser, R. Fricke, J. Chem. Soc. Faraday Trans. 93 (1997) 1849.
[33] H. Kosslick, G. Lischke, B. Parlitz, W. Storek, R. Fricke, Appl. Catal. A 184 (1999) 49.
[34] S.B. Pu, J.B. Kim, M. Seno, T. Inui, Micropor. Mater. 10 (1997) 25.
[35] R.B. Borade, A. Clearfield, Catal. Lett. 31 (1995) 267.
[36] S.K. Badamali, Ph.D. Thesis, IIT Bombay, 1999.
[37] J.S. Beck, J.C. Vartuli, W.J. Roth, M.E. Leonowicz, C.T. Kresge, K.D. Schmitt, C.T.-W. Chu, D.H. Olson, E.W. Sheppard, S.B. McCullen, J.B. Higgins, J.L. Schlenker, J. Am. Chem. Soc. 114 (1992) 10834.
[38] C.T. Kresge, M.E. Leonowicz, W.J. Roth, J.C. Vartuli, J.S. Beck, Nature 359 (1992) 710.
[39] R.D. Shannon, C.T. Prewitt, Acta. Crystallogr. B 25 (1969) 925.
[40] C.-Y. Chen, H.-X. Li, M.E. Davis, Micropor. Mater. 2 (1997) 17.
[41] K.M. Reddy, C. Song, Catal. Lett. 36 (1996) 103.
[42] S.K. Badamali, A. Sakthivel, P. Selvam, in: D.D. Do et al. (Eds.), Proc. Second Pacific Basin Conf. on Ads. Sci. Technol., World Scientific, Singapore, 2000, p. 553.
[43] X.S. Zhao, G.Q. Lu, G.J. Millar, X.S. Li, Catal. Lett. 38 (1995) 33.
[44] Z. Liu, P. Moreau, F. Fajula, Appl. Catal. A 159 (1997) 305.